International Symposium
On Turbulence and Shear Flow
Phenomena (TSFP-9)
June 30 - July 3, 2015 *Melbourne, Australia*

Large Eddy Simulation of Flame Flashback by Combustion Induced Vortex Breakdown

Eike Tangermann
Institut für Mathematik und Rechneranwendung
Universität der Bundeswehr München
W.-Heisenberg-Weg 39, Neubiberg, Germany
eike.tangermann@unibw.de

Markus Klein
Institut für Mathematik und Rechneranwendung
Universität der Bundeswehr München
W.-Heisenberg-Weg 39, Neubiberg, Germany
markus.klein@unibw.de

Michael Pfitzner
Institut für Thermodynamik
Universität der Bundeswehr München
W.-Heisenberg-Weg 39, Neubiberg, Germany
michael.pfitzner@unibw.de

ABSTRACT

Flame flashback is a major concern during the design of lean premixed gas turbine combustors. One particular mechanism of flame flashback in swirl stabilized combustors is the combustion induced vortex breakdown (CIVB), where the flame can propagate upstream against flow velocities far higher than the local turbulent flame speed. In the present work flame flashback by CIVB has been investigated for two combustors of different scale using large eddy simulation. The LES offers full access to a well resolved flow field and allows a detailed analysis of the fluid mechanical processes happening around the flame tip. The method is shown being able to reproduce the operating points limiting stable operation. The analysis of each flashback process then reveals, that the driving mechanism is different for both combustors depending on their size and the swirl velocity field. Either a baroclinic push or a flame propagation by stretching of the flow can be observed.

INTRODUCTION

Lean premixed combustion in gas turbine burners is an effective way to reduce NO_x emissions. However, a major concern is the stability of the combustion process, since ignitable gas is present upstream of the combustion zone bringing the risk of flame flashback, and since the lean flame needs to be prevented from extinction by sophisticated stabilization mechanisms.

Several ways of flame stabilization are common, usually they feature the recirculation of burnt, hot gas to provide activation energy for the ignition of fresh gas. The recirculation can be realized in the wake of a body or by fluid mechanical instabilities like a vortex breakdown, the latter of which has been used in the presently investigated configurations.

The premixed flow enters the burner from a plenum through a swirl generator into a mixing tub, where a perfect mixture of the reactants is achieved in the swirling flow. A vortex breakdown is forced at the entry of the combustion chamber caused by the sudden change in diameter of the confining walls. The thus created recirculation zone transports hot burnt gas upstream igniting the arriving fresh gas.

The vortex breakdown can also be caused by an obstacle located on the centreline. Inside a recirculation zone the flame front can act as such an obstacle and influence the vortex breakdown. The so called combustion induced vortex breakdown (CIVB) has been described by Fritz et al. (2004). If the flame front is located far enough upstream within the swirl tube it can push the vortex breakdown further upstream, which itself pulls the flame even further upstream. The recirculation zone propagates against the flow at a higher velocity than the local turbulent flame speed.

Due to the confinement the experimental access to the propagating flame is very limited. Most of the process takes place inside the mixing tube. By using a silica glass mixing tube optical measurement can be used with some restrictions (Fritz 2004, Konle 2008). The curved surface leads to bending effects of the light and parts of the images are superimposed by reflections and thus become unusable.

Numerical simulation offers a far more detailed view to the flow, each component of the flow field can be accessed at every time step regardless of geometrical restrictions. This allows to deeply analyse the fluid mechanical phenomena and to identify the mechanisms which are the reason of the flame flashback by CIVB.

Several studies have investigated the phenomenon previously to identify the fluid dynamical mechanism of the CIVB. The dominant production terms of circumferential vorticity, which induce the flow deceleration upstream of the vortex breakdown, have been assessed. From the correlation between flashback and swirl velocities observed in his experiments, Fritz (2004) deduces that the stretching around the flame drives the CIVB. Kiesewetter (2005) has performed RANS simulations of the process and extracted the vorticity production terms from CFD data indicating a baroclinic mechanism. From LES of the CIVB in an unconfined vortex Kröger (2010), in agreement with the model by Fritz, shows the stretching around the flame as the dominant term. Kröger (unlike Kiesewetter) has investigated the flow deceleration induced by the production terms, while Kiesewetter only has regarded the local vorticity production.

In the present study two swirl stabilized combustor models without a central body have been investigated using

Large Eddy simulation (LES) with respect to their CIVB behaviour. The two variants differ in the way of swirl generation as well as in the geometrical size. For both the flame flashback by CIVB has been simulated using LES to reveal the fluid dynamical mechanism of the vortex breakdown.

GOVERNING EQUATIONS

The Large Eddy simulations have been performed using the finite volume capabilities of the OpenFOAM code. The flow is described by the density-weighted filtered conservation equations of mass, momentum and enthalpy for a compressible fluid. Momentum and pressure are linked by the PISO algorithm. Subgrid-scale turbulence is modelled with the Smagorinsky model.

The chemical state is characterised by a single reactive scalar $\tilde{c}$, the reaction progress variable, for which a filtered transport equation is solved.

$$\frac{\partial \bar{\rho}\tilde{c}}{\partial t} + \frac{\partial \bar{\rho}\tilde{u}_j\tilde{c}}{\partial x_j} = \frac{\partial}{\partial x_j}\bar{\rho}\bar{D}_{eff,c}\frac{\partial \tilde{c}}{\partial x_j} + \overline{S_c} \qquad (1)$$

Sub-grid turbulent scalar flux is modelled by a gradient hypothesis. The source term $\overline{S_c}$ represents the one-step chemical reaction. For its closure a combustion model featuring fractal assumptions for the flame surface is applied. It is based on the Lindstedt-Vaos (1999) model for RANS and has been transferred to LES methodology in previous work by the authors (Tangermann et al. 2010).

The flame propagates at its turbulent flame speed s_t into unburnt gas. The turbulent flame speed depends on the laminar flame speed s_l and turbulent wrinkling, which is expressed by the flame surface density Σ. Thus the source term becomes

$$\overline{S_c} = \rho_u s_l \Sigma \qquad (2)$$

It is then assumed, that the flame surface density has a fractal shape, i.e. it is self-similar with respect to different turbulent scales. With a fractal dimension of 7/3, which according to Kerstein (1988) is being approached for high values of normalized turbulent fluctuation velocity u'/δ_L, the following formulation for the reaction term results.

$$\begin{aligned}\overline{S_c} &= C_R \rho_u s_l^0 \left(\frac{\Delta}{\eta}\right)^{\frac{1}{3}} \cdot \tilde{c}(1-\tilde{c}) \cdot |\nabla \tilde{c}| \\ &= C_R \rho_u s_l^0 \left(\left(\frac{\nu^3}{\nu_{SGS}^2 \nu + \nu_{SGS}^3} \right)^{\frac{1}{4}} C_S \right) \cdot \tilde{c}(1-\tilde{c}) \cdot |\nabla \tilde{c}|\end{aligned} \qquad (3)$$

The cut-off scales of the fractal model are the LES filter width Δ on the outer side and the Kolmogorov length scale η on the inner side, respectively. The Kolmogorov length scale is modelled using the viscosity ν, the modelled subgrid scale viscosity ν_{SGS} from the turbulence model and the Smagorinsky constant C_S.

Since all of the investigated operating conditions of the combustors are situated in the flame regime of thin reaction zones the smallest scales in the flame can be expected to be of the order of η for unity Lewis number following Peters (2000). The model has been validated in previous work (Tangermann et al, 2010).

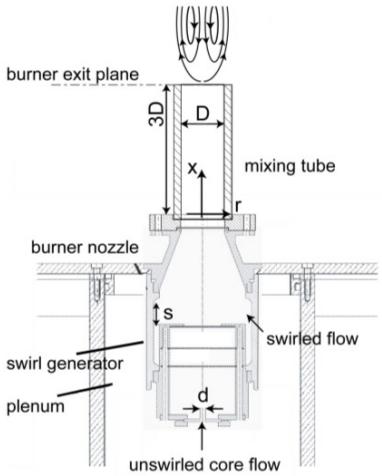

Figure 1. Setup of the TD1 combustor.

The calibration of the model constant C_R to fit the limiting equivalence ratio for flame flashback according to the experiment by Konle (2008) with the TD1 combustor operating at 40kW thermal power setting yields a value of $C_R = 15.0$. This value has been used for the simulation of all cases in the present study.

SMALL SCALE COMBUSTOR

The two gas turbine combustors differ in their size as well as in the method of swirl generation. The first combustor is the TD1 model, which has been investigated by Konle (2008) experimentally. It is the smaller combustor and has a tangential slot swirl generator. The setup is shown in Figure 1. From the plenum premixed gas enters through tangential slots as well as through a non-swirling core jet into the swirl generator. The core jet allows to tune the geometric vortex breakdown characteristics. Downstream of a conical duct is the mixing tube, in which the flame flashback process will be observed. The tube diameter is 40mm and its length is 220mm. At the end of the tube the flow enters the combustion chamber, which has a diameter of 120mm. There a vortex breakdown is occurring already in isothermal conditions. A nozzle has been added at the combustion chamber outlet to ensure numerical stability.

The computational domain resolves the entire combustor including the swirl generator. The core flow is not resolved completely, instead an inlet condition injects 8% of the entire mass flow. This value has been determined by Konle (2008), however, this method implies some uncertainties. The core flow rate strongly influences the axial location of the isothermal vortex breakdown.

Although the flow solver handles the mesh in an unstructured way, the grid is of block structured topology. A square-shaped H-grid along the centreline is surrounded by an O-grid. Two meshes with differently fine resolutions have been used. The coarser one features 2 million cells and a cell width of 1mm in the vortex core region. The finer mesh has a cell width of 0.5mm, which results in 12 million

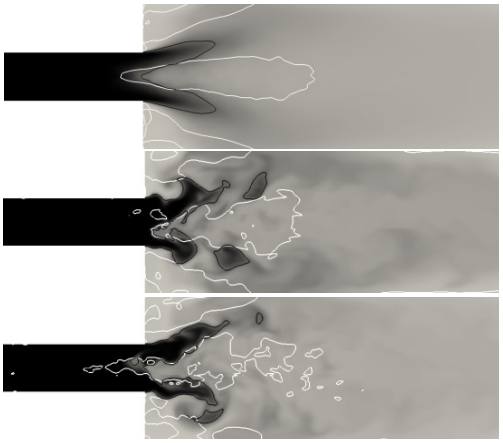

Figure 2. Reaction progress variable field at stable combustion in TD1. Mean flame (top) and instantaneous views. Recirculation zone marked by white isoline.

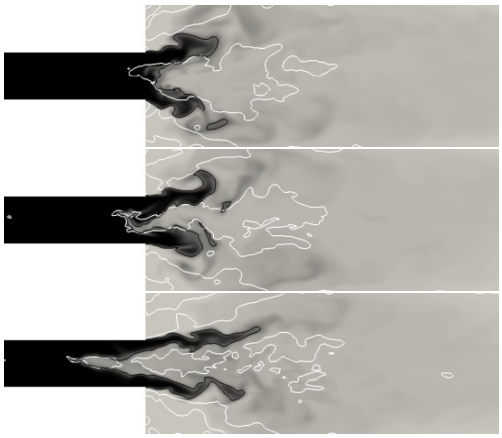

Figure 3. Reaction progress variable field during flame flashback in TD1. Recirculation zone marked by white isoline.

cells. Simulations using the fine grid were performed for one operating point only, while more operating points have been investigated using the coarse grid.

The operating points are defined by the thermal power of the flame, which is 40kW, 60kW and 80kW, respectively. By variation of the air mass flow the equivalence ratio can be tuned from stable operation to flashback, lean blow-out has not been investigated. The equivalence ratio is specified in terms of air excess ratio $\lambda = 1/\varphi$. For each operating point the investigation starts with stable combustion at sufficiently lean conditions. Then as in the experiment the mixture is turned richer stepwise up to flashback. With steps of $\Delta\lambda = 0.05$ a computed time of 0.1s is sufficient to achieve the new stable state or observe flashback.

Prior to the flashback the isothermal flow has been simulated and results were compared to experimental data in order to validate the setup. The swirl profile is in good agreement with the experiment (Konle, 2008) and shows a Burgers-like vortex type. Deviations appear in the axial velocity profile upstream of the vortex breakdown indicating that the breakdown occurs more sudden in the experiment than reproduced by the LES. This might be caused by uncertainties of the core flow boundary condition.

When igniting the mixture at sufficiently lean state (with $\lambda_{\text{flashback}} < \lambda < \lambda_{\text{blowout}}$) a stable flame develops inside the combustion chamber. Figure 2 shows the reaction progress field. The vortex breakdown takes place further upstream than in the isothermal case, indicating that the flame already interferes with the breakdown. In instantaneous views the flame is convected up- and downstream by large scale turbulent structures while the vortex breakdown switches between induction by geometry and by flame depending on the flame position.

Flame flashback analysis. At sufficiently rich mixture conditions the flame always keeps close to the geometrical vortex breakdown and the CIVB becomes dominant. The flame pushes the breakdown position further upstream while being pulled towards the stagnation point itself. The resulting flashback process is illustrated in Figure 3 at three different instances. When the flame has propagated far enough into the mixing tube, a recirculation bubble separates. By the expansion of hot gas within the tube the main recirculation zone is washed out of the tube. Finally it even is transported out of the combustion chamber.

The flashback is a stochastic event, it is influenced strongly by turbulent structures interfering with the flame and with the vortex breakdown. Thus the flashback velocity varies between several observed flashback processes. Figure 4 shows the positions of stagnation point and flame tip before and during the flashback. At 40kW three flame flashback simulations have been performed at different initial instances resulting in different propagation velocities between 1.67m/s and 3.05m/s. Starting from an equivalence ratio of λ=1.70 the flame tip is located well behind the stagnation point. With enriched conditions at λ=1.65 the flame tip first moves closer to the stagnation point before both propagate upstream very suddenly.

The result from the finely resolved simulation is shown in Figure 5 together with experimental results by Konle (2008). The setting of λ=1.55 is situated on the unstable side and immediately after enrichment from stable conditions leads to flame flashback. The comparison shows a good agreement of flashback velocity between experiment and simulation regarding the variation seen before. In the experiment stagnation point and flame tip show a slightly larger distance. However, in the experiment only the locations within a laser cutting plane through the centreline of the mixing tube were considered while the simulation data is based on a fully three-dimensional data processing.

With increasing flame power the mass flow rate increases. The flame has to propagate against higher velocities, thus the flashback occurs at higher equivalence ratios. The critical equivalence ratios have also been determined in the experiments by Konle (2008). At 40kW the combustion model has been calibrated to fit the critical equivalence ratio. At 60kW the flame is predicted more stable with a higher critical equivalence ratio than observed in the experiment. This is probably a result of uncertainties in the model

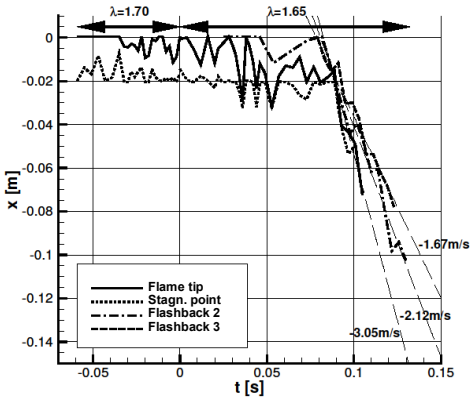

Figure 4. Positions of stagnation point and flame tip during flashback at 40kW power setting with TD1.

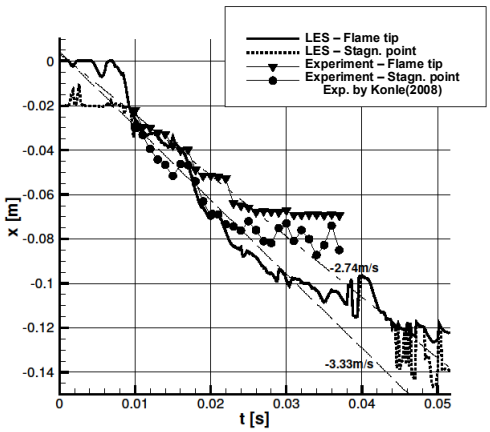

Figure 5. Stagnation point and flame tip during flashback, TD1, high resolution at 40kW λ=1.55.

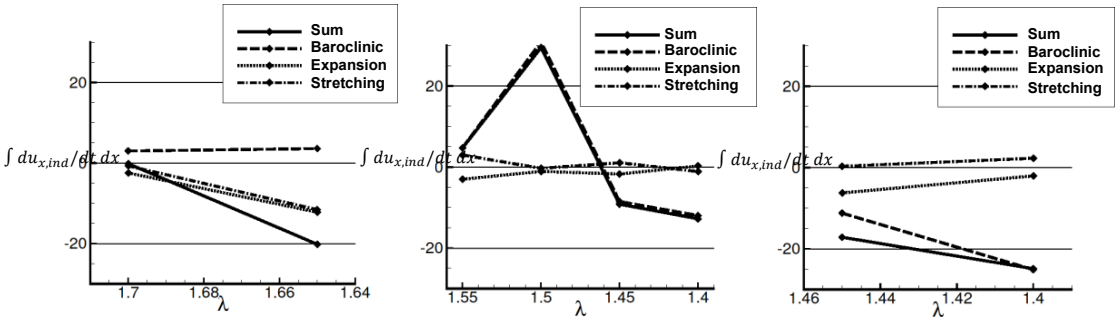

Figure 6. Production of induced axial acceleration. Left to right: 40kW, 60kW, 80kW.

setup, namely the core flow controlling the isothermal vortex breakdown. For 80kW the critical equivalence ratio agrees with the experimental finding.

To identify the induction mechanism of the vortex breakdown in the presence of the flame, a closer look to the vorticity field is necessary. In the compressible vorticity transport equation three source terms arise. The production is fed by stretching of the vortex, volume expansion and baroclinic behaviour.

$$\frac{D\boldsymbol{\omega}}{Dt} = \underbrace{-\boldsymbol{\omega}(\nabla \cdot \boldsymbol{u})}_{expansion} + \underbrace{\frac{1}{\rho^2}\nabla\rho \times \nabla p}_{baroclinic} + \underbrace{(\boldsymbol{\omega} \cdot \nabla)\boldsymbol{u}}_{stretching} \qquad (4)$$

The effect of vorticity on the local induced velocity $\boldsymbol{u}_{ind}$ can be determined by the law of Biot-Savart. Biot-Savart strictly only is valid for incompressible flows, the result should not be considered quantitatively correct. However, for the present application it still gives a good qualitative impression. Differentiating $d\boldsymbol{u}_{ind}/dt$ and inserting equation 4 results in an expression for the local induced acceleration by the different production mechanisms. By analysing the circumferential component of vorticity production, the mechanism can be identified, which leads to the axial deceleration of the flow upstream of the stagnation point and thus to vortex breakdown.

Before the analysis of the source terms the flow field is averaged in several ways. At each time step a circumferential average is built to a quasi-two-dimensional view to reduce computational time, when calculating the Biot-Savart law. Then the temporally fluctuating field is averaged in time with the origin conditioned to the flame tip. The resulting field shows a stationary flame during flashback. The induced acceleration is computed along the centreline of the burner. Finally the resulting acceleration has been integrated along a line spanning half a mixing tube diameter upstream and downstream of the flame tip.

Figure 6 shows in which way the three different mechanisms contribute to the axial velocity deceleration. It reveals, that the mechanism differs between the three investigated power settings. At 40kW the vortex breakdown is driven by stretching and expansion, while the baroclinic term slightly stabilises the flow. The flame is acting like an obstacle and the flow needs to diverge around it.

At the higher power settings of 60kW and 80kW, when also higher velocities are present, the vortex breakdown dominantly is induced by the baroclinic term, while the other two terms are close to zero. For 60kW the baroclinic term at leaner conditions even acts in a stabilising way up to λ=1.50, but then becomes the driving factor. For 80kW the mechanism looks very similar to 60kW, however, the leaner steps have not been simulated, thus the stabilisation by the baroclinic factor does not appear.

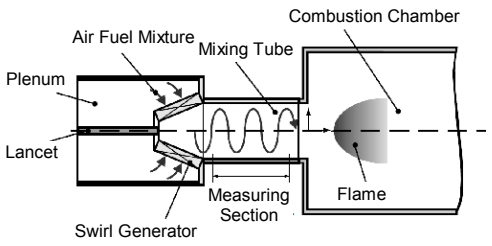

Figure 7. Setup of the BK2 combustor.

FULL SCALE COMBUSTOR

After analysing the laboratory scale TD1 combustor the further investigation is performed in a similar way with a large scale model called BK2 by Fritz (2004). The BK2 features an industrial double-cone swirl generator. With a mixing tube diameter of 75mm, the size is almost double compared to the TD1. Figure 7 shows the setup schematically.

For the numerical simulation the setup has been simplified by omitting the swirl generator. Instead the swirling velocity profile is induced by the inlet boundary condition. The profiles of velocities, Reynolds stresses and turbulent length scale are available from separate computations by Kiesewetter (2003), who also has shown, that skipping the swirl generator is admissible.

An outlet nozzle has been introduced to the simulation domain for numerical stability reasons. The mesh features 2 million cells with a cell width of 0.93mm in radial and 2mm in axial direction within the mixing tube. In the combustion chamber the cells become larger.

At the LES inlet boundary pseudoturbulent velocity fluctuations fitting Reynolds stress and length scale profiles have been superimposed to the mean profiles. The fluctuations have been generated using a method based on diffusing a random field (Kempf et al. 2005). Application to CIVB has been demonstrated in previous work (Tangermann et al. 2008).

Validation of the setup has been performed in a similar way as for the TD1. The isothermal flow shows good agreement with measured data and features a vortex breakdown inside the combustion chamber. Stable combustion already drives the breakdown location slightly into the mixing tube.

Flame flashback analysis. At first sight the flame flashback process appears similar to the one observed at TD1. The flame keeps attached to the stagnation point and both the flame and a separated recirculation bubble propagate upstream until reaching the inlet boundary. Snapshots from instances during the process are shown in Figure 8.

However, a closer look reveals, that the flame flashback here takes place in two phases. The positions of flame tip and stagnation point are plotted in time in Figure 9. At the beginning a very sudden upstream propagation occurs at a high flashback velocity. The regression line indicates a mean propagation velocity of 12.25m/s upstream. After this initial push, which brings the flame about one diameter into

Figure 8. Reaction progress during flame flashback with BK2. Recirculation zone marked by white isoline.

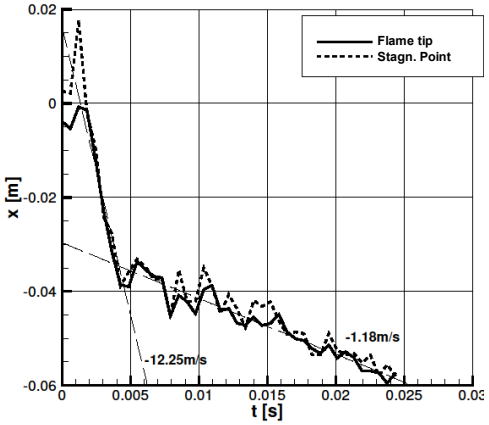

Figure 9. Locations of stagnation point and flame tip during flashback with BK2.

the mixing tube, a phase of slower propagation follows. The propagation velocity drops to 1.18m/s, one tenth of the initial value.

This clear separation into two phases implies a separate analysis of vorticity source terms for each phase. The induced acceleration of each mechanism is shown in Figure 10 along the mixing tube axis. Unlike above it is conditioned to the flame tip and averaged but not integrated. During stable combustion all three mechanisms produce negative axial acceleration. Dominating source is the stretching term, which is already present well before the breakdown zone and initiates the vortex breakdown. The terms of expansion and baroclinic behaviour only occur around the flame tip, since they both are related to density changes.

Then a strong baroclinic push induces the sudden upstream propagation of the flame into the mixing tube. The terms of stretching and expansion remain almost unchanged in relation to the stable operation.

After the decay of the push the baroclinic mechanism reverts to an accelerating source while the further flashback

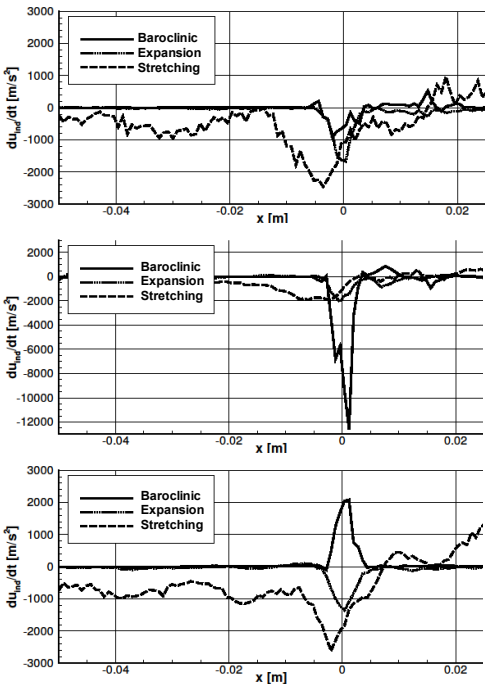

Figure 10. Production of axial acceleration during stable operation (top), initial push (centre) and slow propagation (bottom).

is driven by stretching and expansion. This explains, why the flashback velocity decreases by a factor of ten.

From RANS simulations of the BK2 burner Kiesewetter (2005) concluded the baroclinic term being the driving source for the whole process of flame flashback. However, Kiesewetter did not perform the integration of the Biot-Savart law, but investigated the vorticity production locally.

The conclusion of the present study does not fully support this point of view. But it confirms the results of Fritz (2004), who has found in his experimental study of the same burner a linear correlation between the circumferential velocity and the flashback velocity, indicating that the main cause for the vortex breakdown is in the stretching term. According to Ashurst (1996) a quadratic correlation is to be expected for baroclinically driven flame propagation.

For an unconfined vortex a similar study has been performed by Kröger (2010). It shows a similar behaviour for the flame flashback with the stretching term being dominant during the flashback phase. The baroclinic push in the initial phase could not be shown due to the setup of the unconfined vortex.

CONCLUSIONS

The flame flashback by combustion induced vortex breakdown (CIVB) has been investigated using LES for two different gas turbine model combustors, the laboratory scale TD1 and the more realistic, larger scale BK2. For both burners the flame flashback has been reproduced in good agreement with previous experimental findings.

With the TD1 burner the study covers several operating points, for which stability limits with respect to flame flashback have been determined generally showing agreement with the experiment but also some deviations caused by uncertainties concerning the simplifications met to model the boundary conditions.

By the analysis of vorticity production terms the mechanism of CIVB has been revealed. For the smaller TD1 burner the whole flashback process is dominated by the baroclinic production of circumferential vorticity, which decelerates the flow upstream of the vortex breakdown. In the BK2 burner only the initial phase of the flame flashback is caused by such a baroclinic push. The following phase of slower flame propagation is dominated by the stretching source term, while the baroclinic contribution even stabilises the flow by acceleration.

The difference between both burners can be found partly in the different swirl velocity profiles by the different swirl generators. Another factor is the degree of confinement by the mixing tube as analysis of an unconfined flow by Kröger (2010) indicates.

ACKNOWLEDGEMENT

The authors gratefully acknowledge funding by the DFG (German Research Council).

REFERENCES

Ashurst, W.T., 1996, "Flame propagation along a vortex: The baroclinic push", *Comb. Sci. and Techn., Vol. 112, pp 175-185*

Fritz, J., Kröner, M. and Sattelmayer, T., 2004, „Flashback in a swirl burner with cylindrical premixing zone". *J. of Eng. for Gas Turbines and Power, Vol. 126(2), pp. 267-283*

Kempf, A., Klein, M. and Janicka, J., 2005, „Efficient generation of initial and inflow-conditions for transient flows in arbitrary geometries", *Flow, Turb. and Comb., Vol. 74, pp. 67-84*

Kerstein A., 1988, "Fractal dimension of turbulent premixed flames", *Comb. Sci. and Techn., Vol. 60 pp. 441-445*

Kiesewetter, F., 2005, „Modellierung des verbrennungsinduzierten Wirbelaufplatzens in Vormischbrennern.", *PhD Thesis, TU München*

Konle, M. and Sattelmayer, T., 2008, "Interaction of heat release and vortex breakdown in swirling flame", *14th Int. Symp. on Appl. Laser Techn. to Fluid Mech.*

Kröger, H., Hassel, E., Kornev, N. and Wendig, D., 2010, „LES of premixed flame propagation in a free straight vortex", *Flow, Turb. And Comb., Vol. 84, pp. 513-541*

Peters, N., 2000, "Turbulent Combustion", *Cambridge University Press*, pp. 66-169

Tangermann, E. and Pfitzner, M., 2008, "Numerical investigation of flame flashback into swirling flow", *ASME Paper GT-2008-51081*

Tangermann, E., Keppeler, R., and Pfitzner, M., 2010, "Premixed turbulent combustion models for Large Eddy and RANS Simulations", *ASME Paper GT-2010-22298*